On the streak spacing and vortex roll size in a turbulent channel flow

M. Rajaee,[a] S. Karlsson, and L. Sirovich
Center for Fluid Mechanics, Brown University, Providence, Rhode Island 02912

(Received 28 December 1994; accepted 6 June 1995)

Streamwise high vorticity rolls and streaks in the turbulent channel flows have been the subject of many studies due to their important role in turbulence production, as a result of sweeping, ejection, and bursting of these structures. Understanding the physics of these streamwise structures is important in controlling drag producing events. Investigations of the average streak spacing of the low-speed streaks have resulted in the generally accepted range of $\overline{\lambda^+}=\overline{\lambda}u_\tau/\nu = 100 \pm 20$, where $\overline{\lambda}$ is the mean spanwise spacing between streaks, normalized to the viscous length ν/u_τ. It is also reported,[1,2] for $y^+\leqslant 30$, that the streak spacing grows nearly linearly with distance from the wall. The previous studies mostly have focused on distances close to the wall. Here we report on correlation measurements extended into the log layer, which show that the linear growth of the vortex diameter and the streak spacing extends well in the log layer. Arguments are presented to distinguish these two measures. © *1995 American Institute of Physics.*

I. INTRODUCTION

The subject of drag reduction has drawn the attention of many researchers (see Choi[3] for a comprehensive set of articles; also see Handler *et al.*[4]). The principal has been the focus on control of the inner layer structures, dominated by low-speed streaks, which act as sites for the production of turbulent kinetic energy, a process identified by Kim, Kline, and Reynolds[5] as "bursting." During this process, individual low-speed streaks are described as lifting away from the wall, oscillating, and then breaking down, such that a substantial portion of the low-speed fluid is ejected into the outer flow. An understanding of the physics and geometry of these streaks is essential in order to be able to control or inhibit these drag producing events, or alternately promote them, if an increase in drag is the intention. In this paper we report on basic features of the geometry of streamwise streaks, i.e., streak spacing and vortex roll size, and their variation with wall–normal distance.

The experiments reported here were performed at a moderate Reynolds number channel flow, viz., $R_e=1.22\times10^4$, where R_e is based on the half-channel height and centerline velocity. The roll size and streak spacing are obtained from two-point correlation measurements of the wall–normal and streamwise velocity components measured by two cross-wire miniature probes. It is noteworthy that our correlation measurements are based on long time averages, which in the case of similar measurements in a turbulent boundary layer by Gupta *et al.*[6] did not reveal the streak structure. However, Morrison *et al.*,[7] in their experimental investigations of a turbulent pipe flow, could obtain the streak spacing in the viscous sublayer by the long-time-averaging spectral method. This could be an indication that there are some differences in the near-wall turbulent structures in the boundary layer and the channel flow, or pipe flow. We should note that the driving sources for the turbulence in the two cases are somewhat different in nature, the free-stream kinetic energy in the boundary layer and the flow work of the pressure gradient in the channel or pipe. Also, the boundary layer is a growing flow and the channel, or pipe, flow is not.

It is generally accepted that streak spacing is about 100 ± 20 wall units and that roll width is about 25 wall units (Kim *et al.*,[1] Smith and Metzler,[2] Schraub and Kline,[8] and Oldaker and Tiederman[9]). These results have been collected at wall distances of less than ten wall units. Schraub and Kline[8] showed, using both visual counting and correlation techniques, that the streak spacing increases for $7\leqslant y^+\leqslant20$. Later, Nakagawa and Nezu[10] showed an increase in the mean spacing for ejections and sweeps for $y^+\geqslant10$, asymptoting to a value of $\overline{\lambda^+}\approx 2y^+$ for $y^+>100$. They suggest that the increase in scale may be due to a pairing interaction of the low-speed streaks as they move outward from the wall, resulting in the increase in scale. Studies by Smith and Metzler[2] and Kim, Moin, and Moser[1] also suggest that, for $2\leqslant y^+\leqslant30$, the streak spacing grows linearly with the distance from the wall.

We employ the use of two-point correlations on the streamwise and wall–normal velocity components to estimate the streak spacing and the vortex roll size. Our measurements cover the wall distances of $16.7\leqslant y^+\leqslant104$. These correlation measurements augmented by plausible arguments confirm that roll size and streak spacing grow linearly with the wall distance well into the logarithmic layer.

II. CHANNEL FLOW EXPERIMENTAL SETUP

The channel flow experimental setup is made of a Plexiglas test section that is 28 ft long, 29.5 in. wide (span), and 2.162 in. high. There is a settling chamber prior to the beginning of the test section that is designed to provide a fully developed turbulent flow from the beginning of the channel. This chamber is about 4 ft long, 30.25 in. wide, and 7 in. high. Inside the chamber the top and bottom walls of the channel consist of perforated metal sheets with hole diameters and distribution, such that individual jets are produced, generating an initial flow field with a broad distribution of turbulent fluctuations. The chamber walls are made of ply-

[a]Corresponding author; e-mail: mrj@cfm.brown.edu

 1070-6631/95/7(10)/2439/5/$6.00

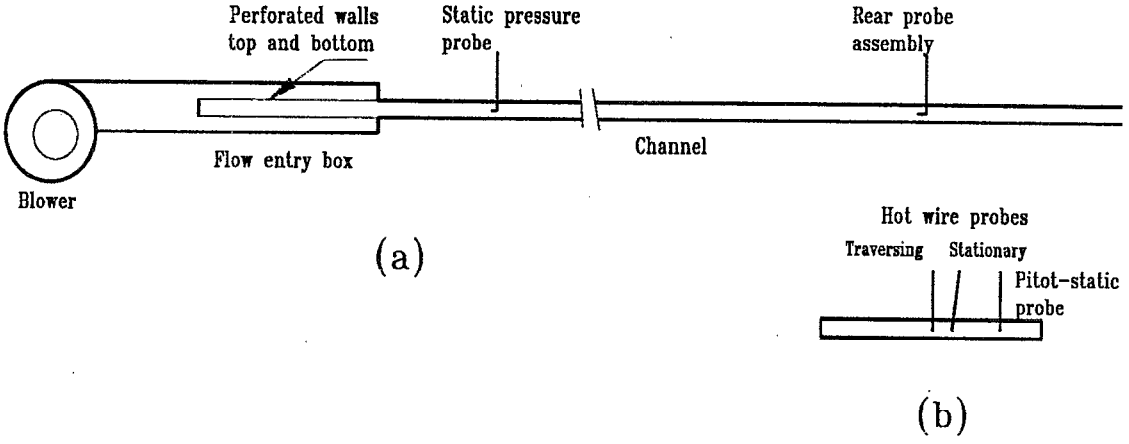

FIG. 1. Schematic of flow system. (a) Side view; (b) end view.

wood. Four aluminum angles mounted on a steel frame support the entire Plexiglas test section and the settling chamber at a height of about 37 in. above the laboratory floor. The steel frame is anchored to the floor and leveled horizontally. It also supports the traversing gear for the hot-wire probes.

The air flow is supplied by a blower with a 4 speed, $\frac{1}{3}$ hp, 6.5 A, motor. The flow enters the chamber through a transition section, made of metal sheets, connecting the chamber to the blower. In addition to the four speed settings of the motor, we can also change the flow rate continuously by adjustable openings of two vents on the transition box sidewalls.

Two component velocity measurements are made by miniature cross-wire probes that are supported by a computer-controlled traversing mechanism allowing hot-wire probe displacements with a 0.0005 in. resolution in both spanwise and wall–normal directions. A Masscomp minicomputer provides high-speed data acquisition from the hot-wire probes. Figure 1 shows the schematic of the channel flow setup.

III. RESULTS AND DISCUSSION

The characteristics of our channel flow are first examined by comparing the velocity profile with the standard profile. For the present setup we find that our flow compares well with the standard turbulent channel flow profile for the channel centerline speeds within the range of 6–10 m/s, which correspond to the flow Reynolds numbers within 10 800–18 000, based on the half-channel width ($h/2$) and the channel centerline velocity. Figure 2 shows the channel flow profile for the mean centerline velocity of 7 m/s. The probes are tilted to measure the flow as close as possible to the bottom wall, and as a result we could not measure very close to the top wall. However, the measurements show a near symmetric profile about the channel centerline. It is compared with the standard turbulent channel profile (Kim *et al.*[1]), corresponding to the skin friction coefficient of C_f=0.0042, as shown in Fig. 3. The measured channel flow profile agrees with the standard profile in the logarithmic layer. The log layer of the standard profile is based on $u^+=2.5 \ln y^+ + 5.5$. For C_f=0.0042, the corresponding friction velocity and viscous length scale become v^*=0.318 m/s and l^*=0.048 mm, respectively.

The pressure gradient in our channel has been determined by measuring the pressure drop between two identical static pressure probes located in the center of the channel at various distances apart in the flow direction. These measurements revealed that the pressure gradient in the flow direction is constant over the region in which the experimental data were collected, verifying that the flow was a fully developed channel flow. From these pressure gradient measurements, the wall skin friction coefficient can be determined, since $\partial P/\partial x=(2/h)\tau_w$ for a fully developed flow in a channel of width h, with a wall shear stress τ_w. Referring to the channel centerline mean velocity, U_c, the skin friction coefficient, C_f, is defined as

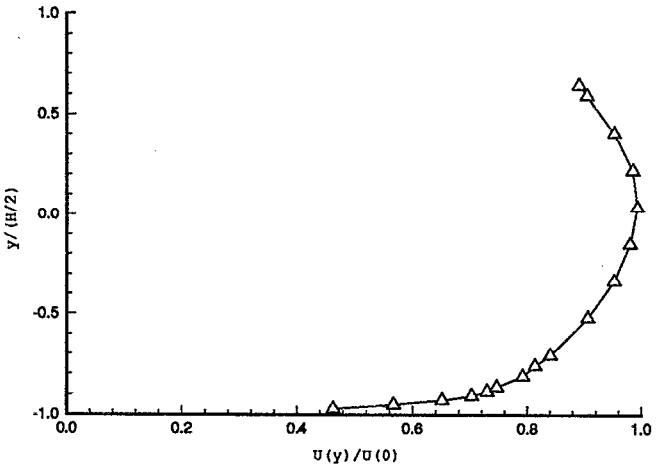

FIG. 2. Channel flow streamwise component velocity profile.

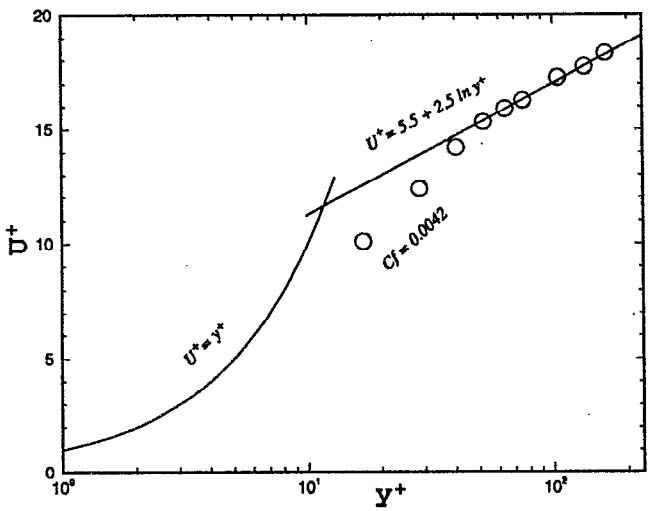

FIG. 3. Comparison of the channel flow profile with the standard profile.

$$C_f=\frac{\tau_w}{\frac{1}{2}\rho U_c^2}=\frac{h(\partial P/\partial x)}{\rho U_c^2}, \tag{1}$$

where ρ=air density. In the experiments reported on here, the pressure gradient was determined from measurements with two static pressure probes 4.493 m apart, and the resulting value for the friction coefficient was $C_f=0.0041$.

For a fully developed two-dimensional turbulent channel flow, one can also relate the wall friction coefficient to the slope of the Reynolds stress in the central portion of the channel,

$$C_f=\frac{h(\partial\overline{uv}/\partial y)}{U_c^2}. \tag{2}$$

In our experiment, $\partial\overline{uv}/\partial y$ was constant over more than 60% of the channel width and could be accurately determined. This method gave a value of $C_f=0.0040$, which is in satisfactory agreement with the value determined from pressure gradient measurements.

We use two cross-wire probes to measure two-point velocity correlations in order to estimate the average roll diameter and the average spanwise spacing between the streaks. One probe, as the reference, is stationed at a fixed location, and the other is traversed in the spanwise direction relative to the first one. Both probes are kept at the same streamwise and wall–normal positions. Instantaneous two-component velocity measurements are made by both probes providing two-point correlations of streamwise and wall–normal velocities.

The only sensible systematic error involved in the measurements is the effect of air temperature change, which could result in an error in the velocity readings by the hot-wire sensors. With an air temperature change range of ±0.5 °C during the measurements, the inaccuracy of velocity measurements is less than 1% of the channel centerline velocity. This source of error is even less important in correlation measurements.

Based on actual measurements, we found that a reliable estimate of mean flow velocity in our turbulent channel flow would require 120 000 data samples, amounting to 120 s of recording at the rate of 1000 samples per second. We tried other sampling rates as high as 4000 samples per second, and we did not observe any sensible change in the time-average correlation and mean flow velocity measurements. In our investigation for the proper length of time for averaging the flow quantities, a further increase of the averaging time to even 10 min showed no sensible change in the mean flow velocity or in the velocity correlation values. The uncertainty of 2 min long-time average of velocity measurements is ±0.3%. In the correlation measurements the mean flow is subtracted from the total u and v measurements. The remainder is the total fluctuating velocity component. If there is any fixed location coherent structure, it will be included in the mean flow, which has been subtracted out, leaving the instantaneous wall layer structures' contribution. The instantaneous velocity fluctuations is then used for velocity correlations. The correlation measurements reveal an average estimate of the roll-like structures' size and spacings based on the analytical reasons discussed later in this section.

The length of sensing element, in the velocity measurements, is of major concern when probing near-wall motions. Blackwelder and Haritonidis[11] suggested that the sensor length $l\leqslant 20\times\lambda$ for hot wires, where λ is the viscous length scale. Therefore, for our flow we should employ sensors with the length of $l=0.97$ mm or smaller. We use miniature hot-wire cross probes with the sensor length of 1 mm, which comes very close to satisfying this requirement.

The probes can measure the flow velocity as close as 0.8 mm, $y^+=16.7$, from the wall. In the series of experiments the wall–normal distance varied over a broad range, viz., $16.7\leqslant y^+\leqslant 104$.

Figure 4(a) shows the two-point correlation of the streamwise velocity component in the spanwise direction at $y^+=16.7$ and 73. The correlations become negative and reach minima at $\Delta z^+\approx 75$ and 304. A curve fitting scheme has been employed for a more accurate estimate of the location of the local minimum in the velocity correlation plots. Likewise, Fig. 4(b) shows the two-point velocity correlation of the wall–normal velocity component at $y^+=37.5$ and 53. In this instance, the minima are located at $\Delta z^+\approx 56$ and 84. In order to explain these curves and to draw physical significance from these results, we adopt a plausible picture of wall bounded turbulent flow. From the broad range of simulations and experiments, we learn that the wall region is dominated by a flow composed of a repeating pattern counter-rotating vortical structures showing little streamwise dependence. If the full velocity is $\mathbf{u}'(\mathbf{x},t)$, then we may write

$$\mathbf{u}'(\mathbf{x},t)=U(y)\mathbf{e}_x+\mathbf{u}(\mathbf{x},t), \tag{3}$$

where $U(y)$ is the mean flow, $\mathbf{e}_x$ is the unit vector, and $\mathbf{u}(\mathbf{x},t)$ is the fluctuation velocity. The measured correlations are given by

$$R_{uu}(y;z-z')=\langle u(x,y,z,t)u(x,y,z',t)\rangle \tag{4}$$

and

$$R_{vv}(y;z-z')=\langle v(x,y,z,t)v(x,y,z',t)\rangle. \tag{5}$$

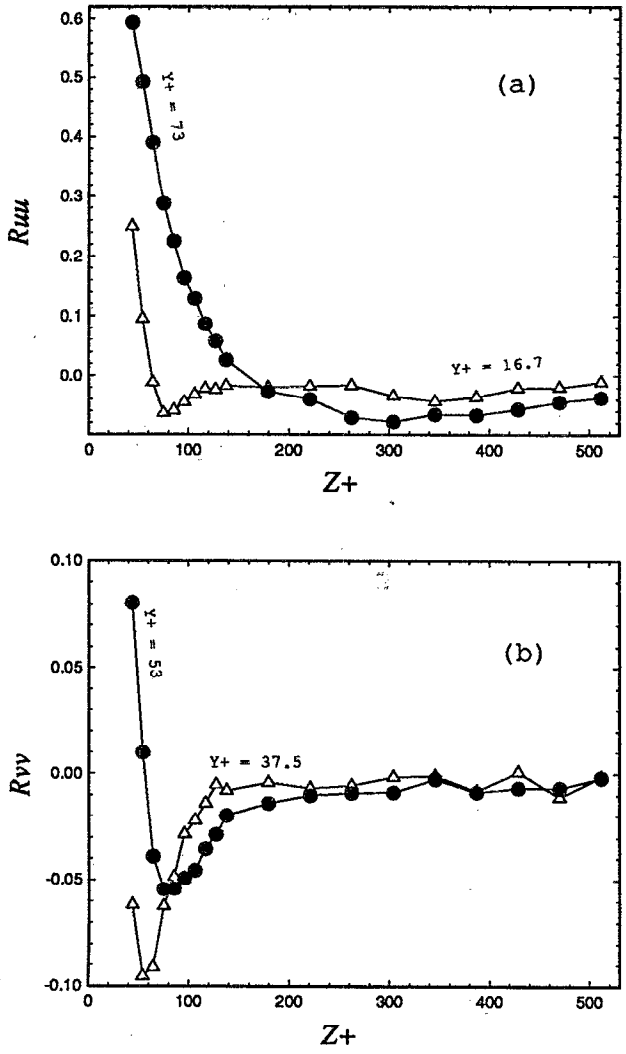

FIG. 4. (a) Two-point correlation of streamwise velocity at $Y^+=16.7$ and 73; (b) two-point correlation of normal velocity at $Y^+=37.5$ and 53.

For the case being considered here, viz. channel flow, these quantities exhibit no streamwise dependence, but a slow x dependence appears in boundary layer flow. We assume an infinite extent in the spanwise coordinate from which it follows that the correlations are translationally invariant, hence the reduction to $z-z'$. If we decompose the fluctuation velocity in the streamwise direction,

$$\mathbf{u}(\mathbf{x},t)=\mathbf{u}_0(y,z,t)+\sum_k e^{ikx}\mathbf{u}_k(y,z,t), \tag{6}$$

then we observe that the first term accounts for the roll-like or vortical structures. As has been pointed out (Sirovich *et al.*[12] and Ball *et al.*[13]), numerical simulations indicate that the second term in (6) is small compared to $\mathbf{u}_0$. Therefore, for purposes of analyzing (4) and (5), we can write

$$\mathbf{u}\approx\mathbf{u}_0(y,z). \tag{7}$$

We can therefore write to good approximation that

$$R_{uu}(y;z-z')\approx\langle u_0(y,z,t)u_0(y,z',t)\rangle, \tag{8}$$

and similarly,

$$R_{vv}(y;z-z')\approx\langle v_0(y,z,t)v_0(y,z',t)\rangle. \tag{9}$$

The curves shown in Fig. 4(b) can now be explained. The minimum (anti)correlation corresponds to a probe separation that is the inner core separation in a single vortex roll. Kim *et al.*[1] present a similar argument to explain the minimum of R_{vv}. To explain the R_{uu} curve we observe that $\mathbf{u}_0$ has a nonzero streamwise component, even though it has no streamwise dependence, but since the net streamwise flux of $\mathbf{u}_0$ must vanish, adjacent rolls have antiparallel counterflowing streamwise velocities. Thus, the minima seen in Fig. 4(a) indicate that the two probes are a half-wavelength apart in each instance. That is, the "streak spacing" is two times the measured distance to the R_{uu} minimum.

Since the actual location of wall streaks is random, one can question how much of the instantaneous structure is revealed by two-point correlation measurements. Toward this end, consider, for example, the flow

$$(u,v,w)=\{U(y)\sin[z-r(t)],\quad V(y)\cos[z-r(t)],\quad -V'(y)\sin[z-r(t)]\}, \tag{10}$$

which clearly satisfies the continuity equation. The forms of $U(y)$ and $V(y)$ are immaterial. Here $r(t)$ is to be thought of as a random variable. Thus, this depicts a flow made up of an endless sequence of counter-rotating, counter flowing rolls and randomly moving side to side. Roll location is random in time and spanwise roll location has uniform probability. Nevertheless, as the simple transformation $z-r(t)\to z$ shows, both $R_{uu}(z)$ and $R_{vv}(z)$ are determined independently of the randomness, and, in particular, the first minimum occurs at a half-wavelength.

This simple model is not rich enough to capture the disparate minima of $R_{uu}(z)$ and $R_{vv}(z)$ seen in the experiments. To obtain this we require counterflowing concentrated rolls that are separated from one another. In this case, the first minima of R_{vv} measures the roll size and that of R_{uu} the roll separation. Such a model should be regarded as a guide to understanding. The actual structures are far more complex. Streak spacing is itself a variable, and if this is introduced into the model, only one sensible minimum will be observed. And as is obvious from simulations (Refs. 14 and 15) and experiments (Refs. 16 and 17) the roll-like structures are three dimensional, i.e., they are not entirely aligned along streamwise direction and they are of finite length.

The picture just presented is largely supported by the Karhunen–Loève (KL) empirical eigenfunction decomposition of channel flow (Refs. 13 and 18). That analysis shows that the streamwise velocity is the largest component of the perturbation. This is in agreement with the well-known experimental result, that the peak $u_{\rm rms}$ is significantly larger than the other components. This then suggests that adjacent rolls are counter-rotating counterflowing jet-like structures. In more detail, we point out that the presence of two scales implies a superposition of KL roll modes, and the finite length of streaks implies that streamwise-dependent KL modes must be included in the description. The need for a

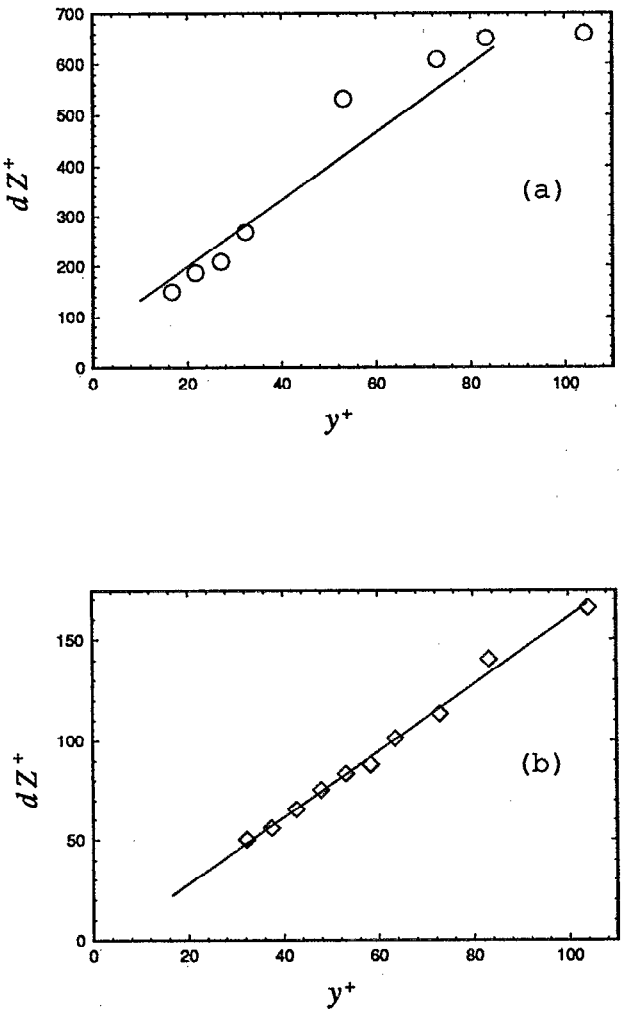

FIG. 5. (a) Mean average streak spacing versus the wall distance; (b) mean diameter of the streamwise vortex versus the wall distance.

time-varying collection of KL modes in the description of coherent structures is more fully described elsewhere (Ref. 19).

Finally, we remark that outside the laminar sublayer $y \gg l_*$ no natural length scale exists, and on dimensional grounds we may write, for example,

$$\langle \mathbf{u}(x,y,z)\mathbf{u}^+(x',y,z')\rangle = \mathbf{R}\left(\frac{x-x'}{y}, \frac{z-z'}{y}\right). \tag{11}$$

This accounts for the linear growth of scales we have found and described below.

The correlation measurements were performed for several wall normal distances within $y^+ = 16.7$ to 104, covering the buffer and logarithmic regions. For the first three experiments at the lower end of the y^+ range we were unable to move the probes close enough to capture the local minimum in the normal velocity correlation plot, indicating that the vortex width is smaller than the minimum attainable probe spacing. Also, at some of the wall distances, $33 \leqslant y^+ \leqslant 52$, we were unable to determine a reliable local minimum in the streamwise correlation plots due to the broadness of the minimum in the correlation curve. However, minima in the normal velocity correlation are clearly identifiable, verifying the remaining presence of a coherent component of longitudinal vortices. At larger y^+ a well-defined minimum in the streamwise correlation reappears.

Figures 5(a) and 5(b) show the estimates of streak spacing and the mean vortex diameter, respectively, versus the wall distances. Figure 5(b) clearly confirms the assertion of linear growth of the vortex diameter, as does Fig. 5(a) for the streak spacing in the wall normal direction.

ACKNOWLEDGMENTS

This work was supported by ORLEV under Contract No. 529584, and we are grateful to E. Levich and L. Y. Bronicki for their support and encouragement.

[1] J. Kim, P. Moin, and R. Moser, "Turbulence statistics in fully developed channel flow at low Reynolds number," J. Fluid Mech. **177**, 133 (1987).
[2] C. R. Smith and S. P. Metzler, "The characteristics of low-speed streaks in the near-wall region of a turbulent boundary layer," J. Fluid Mech. **129**, 27 (1983).
[3] K.-S. Choi, "Recent developments in turbulence management," *Proceedings of the 5th Drag Reduction in Engineering Flows Meeting* (Kluwer, New York, 1991).
[4] R. A. Handler, E. Levich, and L. Sirovich, "Drag reduction in turbulent channel flow by phase randomization," Phys. Fluids A **5**, 686 (1993).
[5] H. T. Kim, S. J. Kline, and W. C. Reynolds, "The production of turbulence near a smooth wall in a turbulent boundary layer," J. Fluid Mech. **50**, 133 (1971).
[6] A. K. Gupta, L. Laufer, and R. E. Kaplan, "Spatial structure in the viscous sublayer." J. Fluid Mech. **50**, 493 (1971).
[7] W. R. B. Morrison, K. J. Bullock, and R. E. Kronauer, "Experimental evidence of waves in the sublayer," J. Fluid Mech. **47**, 639 (1971).
[8] F. A. Schraub and S. J. Kline, "Study of the structure of the turbulent boundary layer with and without longitudinal pressure gradients," Department of Mechanical Engineering, Stanford University, Report No. MD-12, 1965.
[9] L. K. Oldaker and W. G. Tiederman, "Spatial structure of the viscous sublayer in drag reducing channel flows," Phys. Fluids Suppl. II **20**, S133 (1977).
[10] H. Nakagawa and I. Nezu, "Structure of space-time correlations of bursting phenomena in an open-channel flow," J. Fluid Mech. **104**, 1 (1981).
[11] R. F. Blackwelder and J. H. Haritonidis, "Scaling of the bursting frequency in turbulent boundary layers," J. Fluid Mech. **132**, 87 (1983).
[12] L. Sirovich, K. S. Ball, and L. R. Keefe, "Plane waves and structures in turbulent channel flow," Phys. Fluids A **2**, 2217 (1990).
[13] K. S. Ball, L. Sirovich, and L. R. Keefe, "Dynamical eigenfunction decomposition of turbulent channel flow," Int. J. Num. Methods Fluids **12**, 585 (1991).
[14] P. S. Bernard, J. T. Thomas, and R. A. Handler, "Vortex dynamics and the production of Reynolds stress," J. Fluid Mech. **253**, 385 (1993).
[15] S. K. Robinson, "The kinematics of turbulent boundary layer structures," NASA Technical Memorandum 103859, 1991.
[16] C. R. Smith and L. J. Lu, "The use of a template-matching technique to identify hairpin vortex flow structures in turbulent boundary layers," in *Near Wall Turbulence, Proceedings of the Zaric Memorial Conference, 1988*, edited by S. J. Kline and N. H. Afgan (Hemisphere, New York, 1989), p. 248.
[17] J. F. Foss and J. M. Wallace, "The measurement of vorticity in transitional and fully developed turbulent flows," *Frontiers in Experimental Fluid Mechanics* (Springer-Verlag, Berlin, 1989).
[18] L. Sirovich, K. S. Ball, and R. A. Handler, "Propagating structures in wall-bounded turbulent flows." Theor. Comput. Fluid Dyn. **2**, 307 (1991).
[19] L. Sirovich, "Chaotic dynamics of coherent structures," Physica D **37**, 126 (1989).